

Supporting Information

Facile Decoration of Multiwalled Carbon Nanotubes with Hetero-oligophenylene Stabilized-Gold Nanoparticles: Visible Light Photocatalytic Degradation of Rhodamine B Dye

Sharanjeet Kaur, Vandana Bhalla,* and Manoj Kumar*

*Department of chemistry, UGC Center for Advanced Studies Guru Nanak Dev University,
Amritsar, INDIA-143005*

*E-mail: vanmanan@yahoo.co.in, mksharmaa@yahoo.co.in

Page No. Contents

- S-2 to S-4** ^1H , ^{13}C NMR and Mass spectra of derivative **3**.
- S-5** Fluorescence spectra of derivative **3** in different H_2O /TEG mixture and scanning electronic microscopy image of derivative **3** in H_2O : CH_3CN mixture.
- S-6** Dynamic light scattering studies of derivative **3** in H_2O / CH_3CN (6/4) mixture and ratiometric combinational curve I_{485}/I_{355} as a function of $[\text{Au}^{3+}]$ increased.
- S-7** Overlay ^1H NMR spectrum of derivative **3** in presence of 10 eq. of Au^{3+} ions in $\text{CDCl}_3/\text{CD}_3\text{OD}/\text{D}_2\text{O}$ (1:6:3).
- S-8** Calibration curve for Au^{3+} (μM) over the range of 0 – 75 μM of Au^{3+} and detection limit plot of derivative **3** for Au^{3+} ions.
- S-9** Fluorescence emission spectra of derivative **3** in presence of various metal chloride/perchlorate in H_2O / CH_3CN (6/4) mixture and overlay ^1H NMR spectrum of derivative **3** in presence of 10 eq. of Au^{3+} ions in $\text{CDCl}_3/\text{CD}_3\text{OD}/\text{D}_2\text{O}$ (1:6:3).
- S-10** Fluorescence life time decay profile of derivative **3** in CH_3CN and H_2O / CH_3CN (5/5) mixture.
- S-11** Overlay ^1H NMR spectra of derivative **3** in CDCl_3 and organic part obtained after washing in-situ generated gold nanoparticles.
- S-12** UV-vis spectra of derivative **3** in presence of Au^{3+} ions in CH_3CN and fluorescence emission spectra of derivative **3** in presence of tery-butyl hydroperoxide in H_2O : CH_3CN (6:4) mixture.
- S-13** Dynamic light scattering analysis of gold nanoparticles and absorption spectra of the supernatants obtained from three subsequent washing steps in the preparation of AuNPs@MWCNTs nanohybrid materials.
- S-14** UV-vis spectra of gold nanoparticles before and after they are adsorbed onto the surface of multi walled carbon nanotubes and fluorescence emission spectra of AuNPs@MWCNTs nanohybrid materials.
- S-15** TEM images of AuNPs@MWCNTs nanohybrid and FT-IR spectra of derivative **3**, derivative **3** stablized AuNPs and AuNPs@MWCNTs hybrid.

S-16 Pseudo-first-order kinetic for the photodegradation of RhB over AuNPs@MWCNTs and dye adsorption efficiency and photocatalytic efficiency of the recycled AuNPs@MWCNTs nanocatalyst to RhB.

S-17 TEM images of the AuNPs@MWCNTs nanohybrid catalyst after three runs of photocatalytic degradation of RhB and table showing fluorescence lifetime of derivative **3** in absence and presence of Au³⁺ ions (15 equiv) in H₂O/CH₃CN (6:4, v/v).

S-18 Comparison of present method over other reported procedure in literature for the preparation of AuNPs@MWCNTs nanohybrid materials.

S-19 Comparison of catalytic efficiency of AuNPs@MWCNTs nanohybrid materials for photocatalytic degradation of RhB reported in present manuscript with other catalytic systems in the literature.

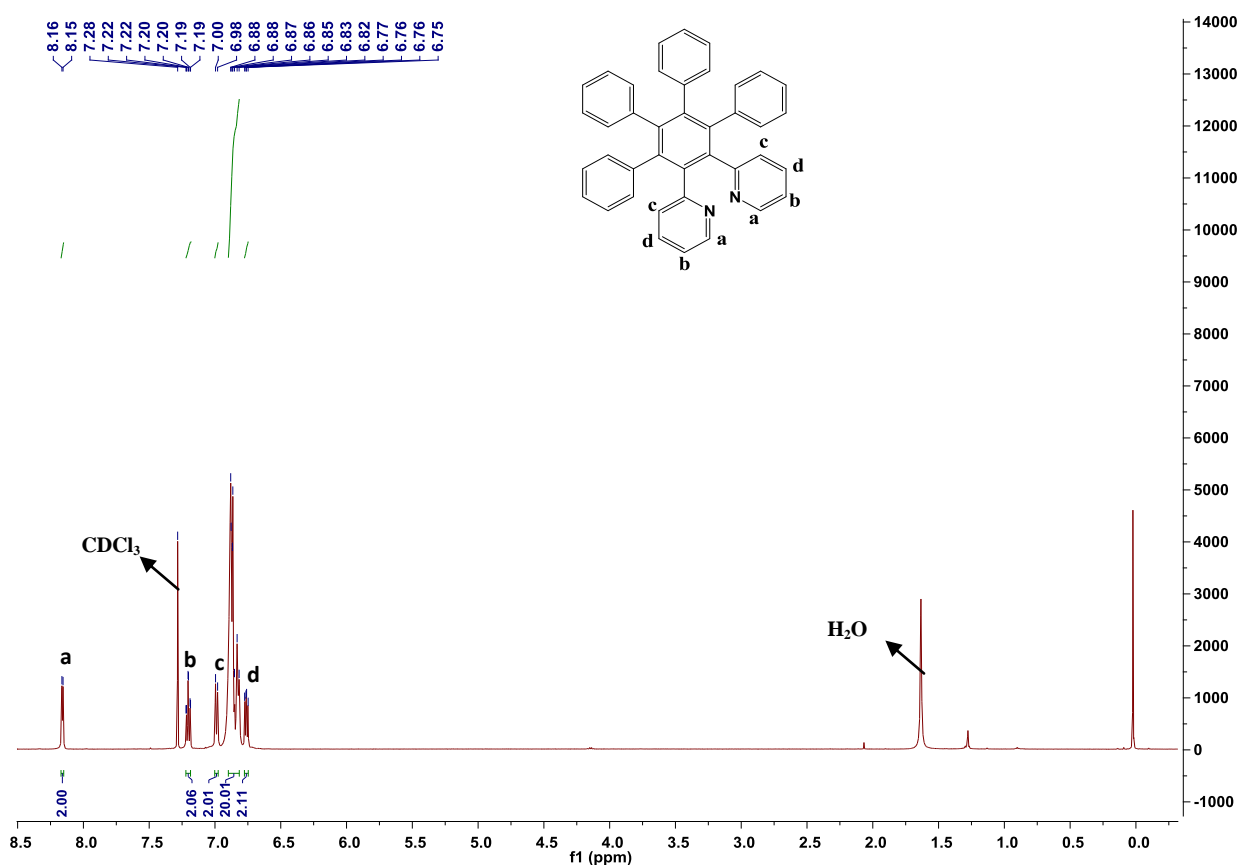


Fig. S1 ¹H NMR spectrum of derivative **3** (500 MHz, CDCl₃)

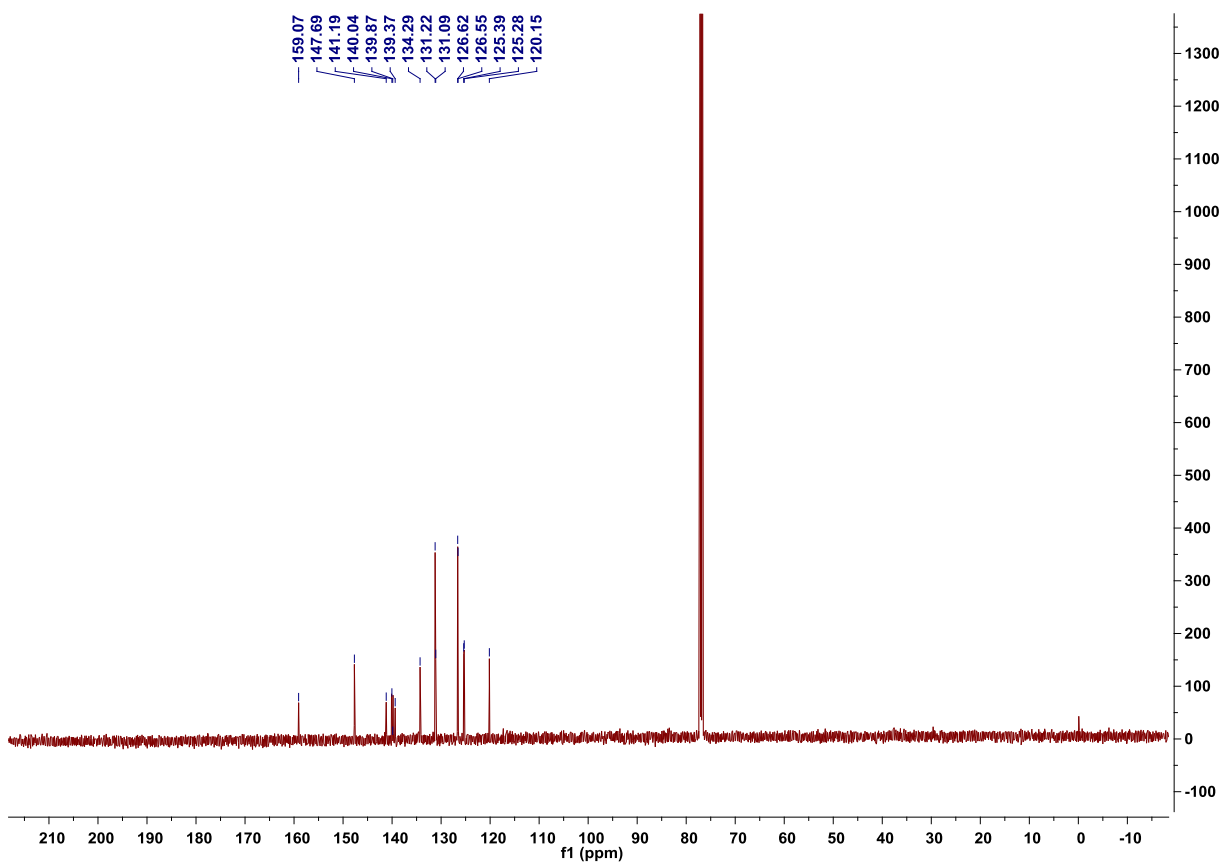


Fig. S2 ¹³C NMR spectrum of derivative **3** (75 MHz, CDCl₃)

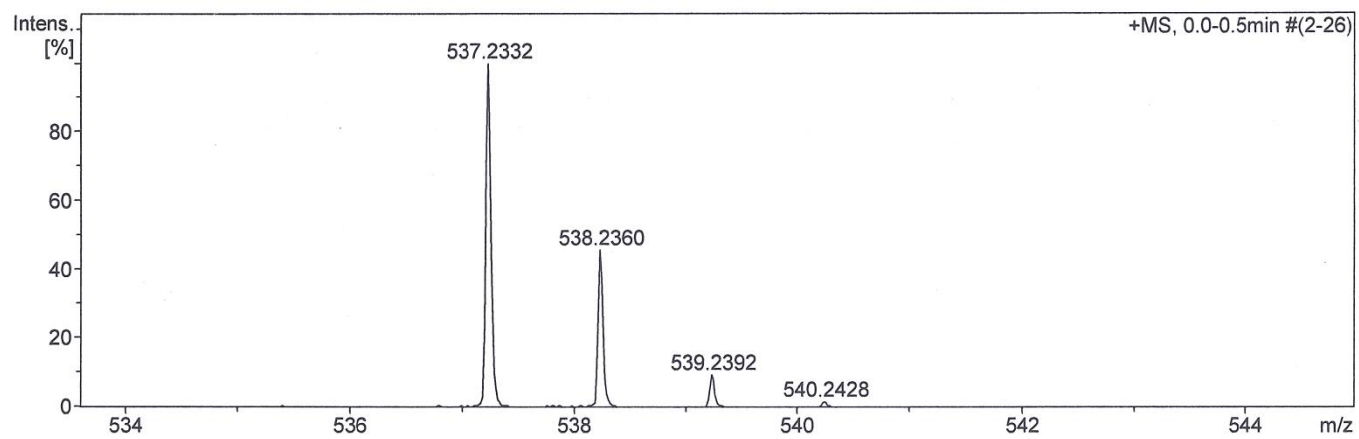
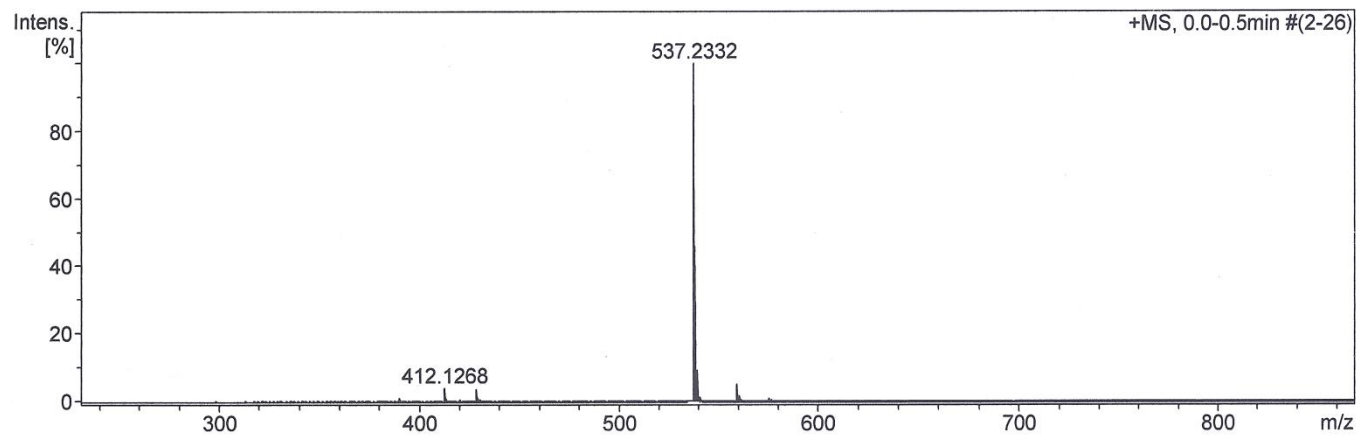


Figure S3 Mass spectrum of derivative **3**.

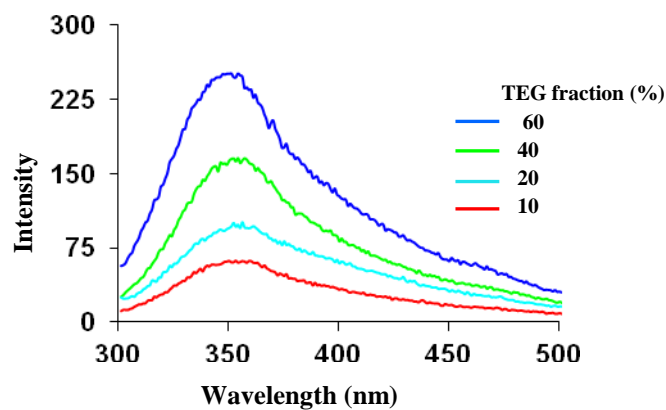


Fig. 4 Fluorescence spectra of compound **3** (5 μ M) showing the variation of fluorescence intensity in TEG/ CH_3CN mixture (0 to 60% volume fraction of TEG in acetonitrile); λ_{ex} = 290 nm.

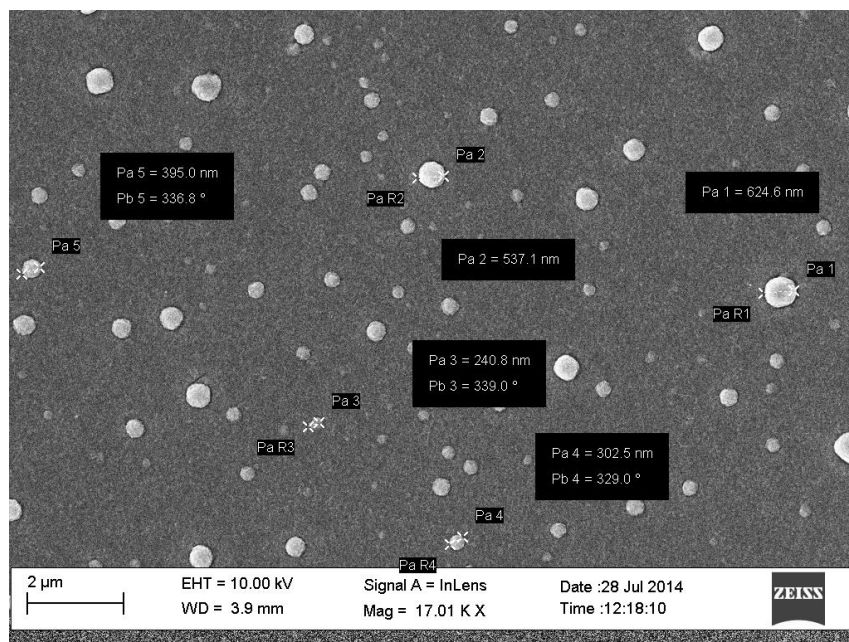


Fig. S5 SEM image of aggregates of compound **3** in $\text{H}_2\text{O}/\text{CH}_3\text{CN}$ (6:4) mixture.

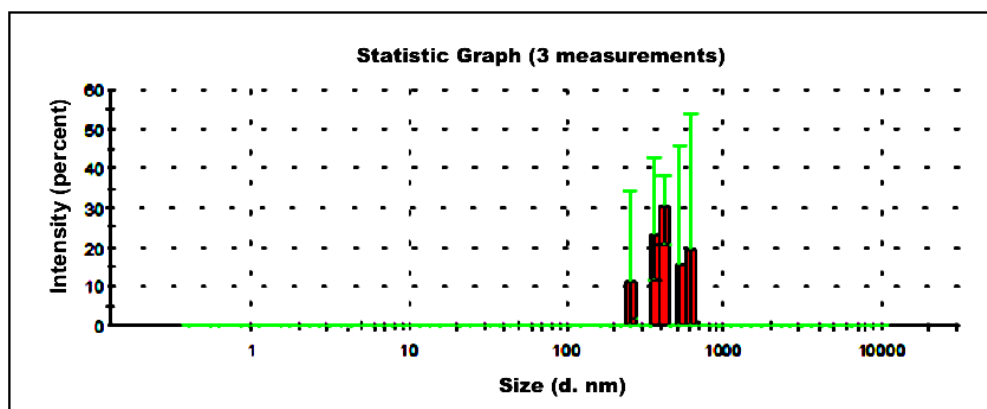


Fig. S6 The dynamic light scattering (DLS) studies derivative **3** showing the average diameter of aggregates is in the range of 500 nm in H₂O/CH₃CN (6/4).

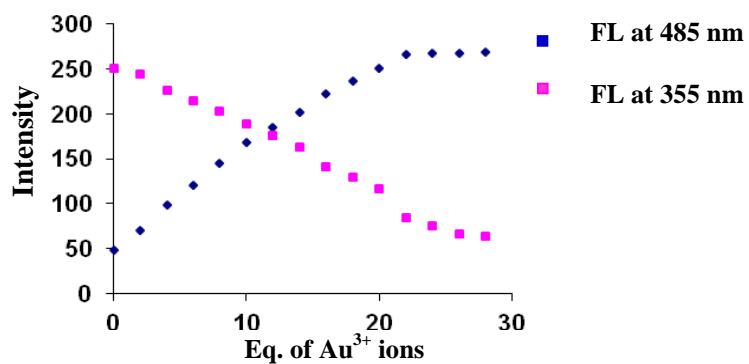


Fig. S7 Ratiometric combinational curve I_{485} (blue) and I_{355} (pink) as a function of $[Au^{3+}]$ increased.

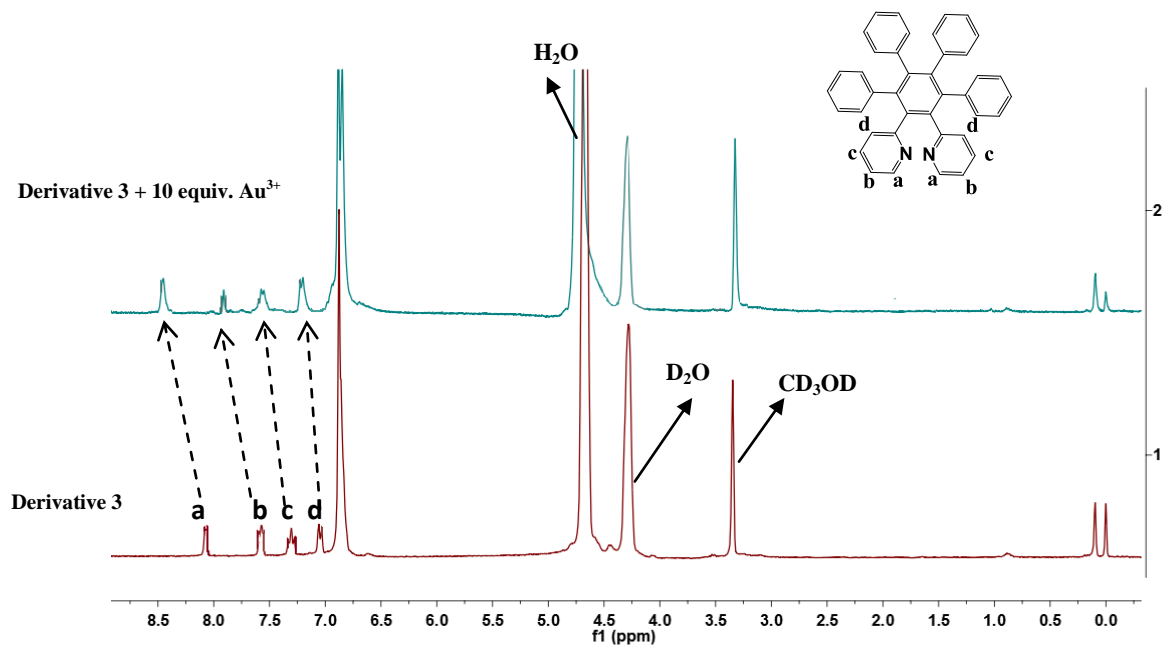


Fig. S8a ^1H NMR titration of compound **3** with Au^{3+} ions in $\text{CDCl}_3/\text{CD}_3\text{OD}/\text{D}_2\text{O}$ (1:6:3).

Derivative 3 (δ_1 ppm)	3 + 10 equiv. Au^{3+} (δ_2 ppm)	$\Delta\delta = \delta_1 - \delta_2$
8.1 (d, 2H, ArH) (a)	8.5 (d)	0.4
7.52-7.6 (m, 2H, ArH) (b)	7.7-7.78 (m)	0.18
7.3-7.39 (m, 2H, ArH) (c)	7.49-7.55 (m)	0.19
7.12 (d, 2H, ArH) (d)	7.23 (d)	0.11

Fig. S8b Change in chemical shift (δ) value of compound **3** before and after addition of Au^{3+} ions in $\text{CDCl}_3/\text{CD}_3\text{OD}/\text{D}_2\text{O}$ (1:6:3).

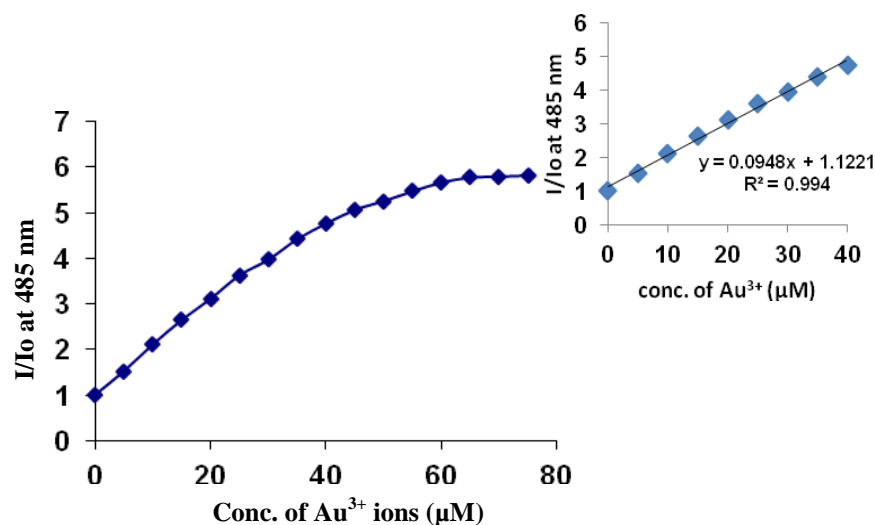


Fig. S9 Calibration curve for Au^{3+} (μM) over the range of 0 – 75 μM of Au^{3+} . Inset the fluorescence intensity of derivative **3** at 485 nm showed a linear response to Au^{3+} in the concentration range of 0 to 40 μM .

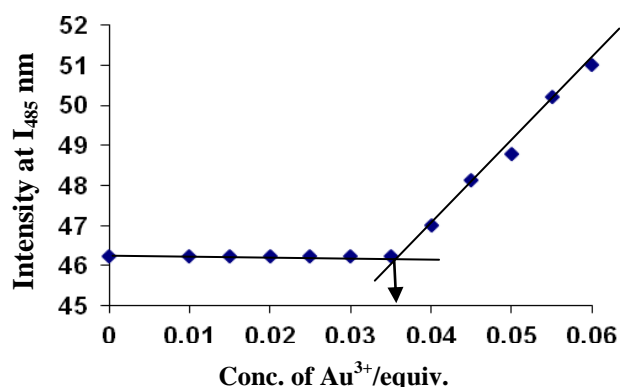


Fig. S10 Showing the fluorescence intensity of derivative **3** at 485 nm as a function of Au^{3+} ions concentration (equiv.) in $\text{H}_2\text{O}/\text{CH}_3\text{CN}$ (6:4, v/v), $\lambda_{\text{ex}} = 300$ nm.

To determine the detection limit, fluorescence titration of compound **3** with Au^{3+} ions was carried out by adding aliquots of gold solution (in equiv.) and the fluorescence intensity as a function of Au^{3+} ions added was then plotted. From this graph the concentration at which there was a sharp change in the fluorescence intensity multiplied with the concentration of receptor **3** gave the detection limit.

Equation used for calculating detection limit (DL):

$$\text{DL} = \text{CL} \times \text{CT}$$

CL = Conc. of Ligand; CT = Conc. of Titrant at which change observed.

Detection limit (DL) of Au^{3+} ions with **3:**

$$\text{Thus; DL} = 0.036 \times 10^{-6} = 36 \times 10^{-9} = 36 \text{ nM.}$$

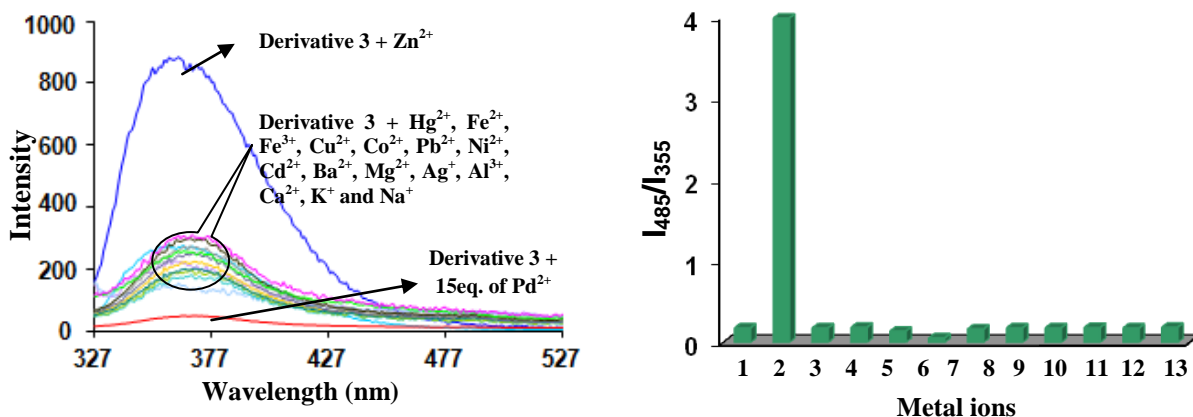


Fig. S11 Fluorescence emission spectra of derivative **3** (5 μM) with the addition of different metal ions (25 equiv.) in $\text{H}_2\text{O}/\text{CH}_3\text{CN}$ (6:4), buffered with HEPES pH = 7.2 (B) Fluorescence selectivity (I_{490}/I_{363}) of **3** (5 μM) in the presence of various metal ions (25 equiv each); 1 = Hg^{2+} , 2 = Co^{2+} , 3 = Pb^{2+} , 4 = Ni^{2+} , 5 = Cd^{2+} , 6 = Pd^{2+} , 7 = Zn^{2+} , 8 = Cu^{2+} , 9 = Ba^{2+} , 10 = Mg^{2+} , 11 = K^+ , 12 = Na^+ , and 13 = Li^+

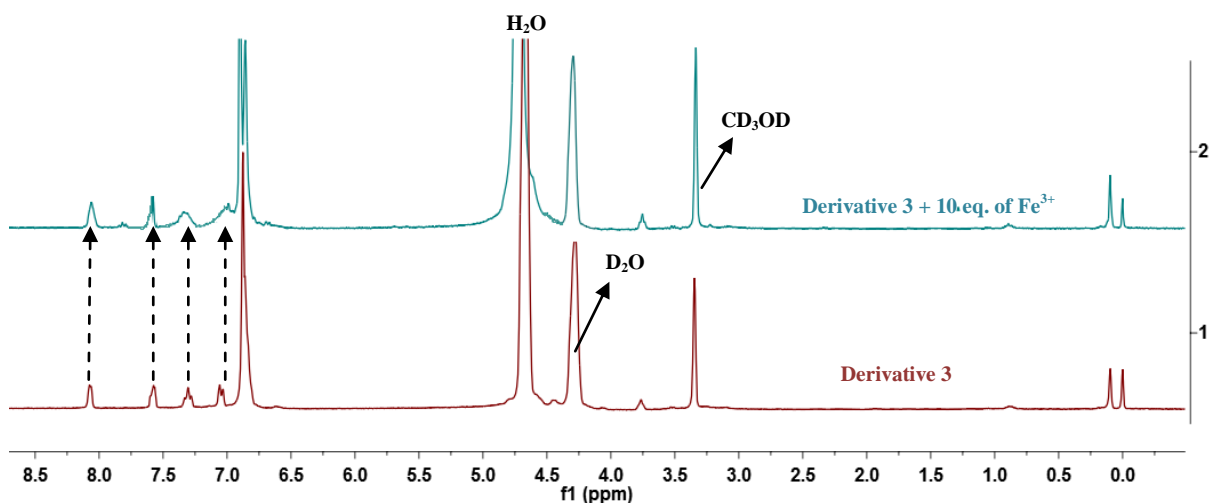


Fig. S12 ^1H NMR titration of compound **3** with Fe^{3+} ions in $\text{CDCl}_3/\text{CD}_3\text{OD}/\text{D}_2\text{O}$ (1:6:3).

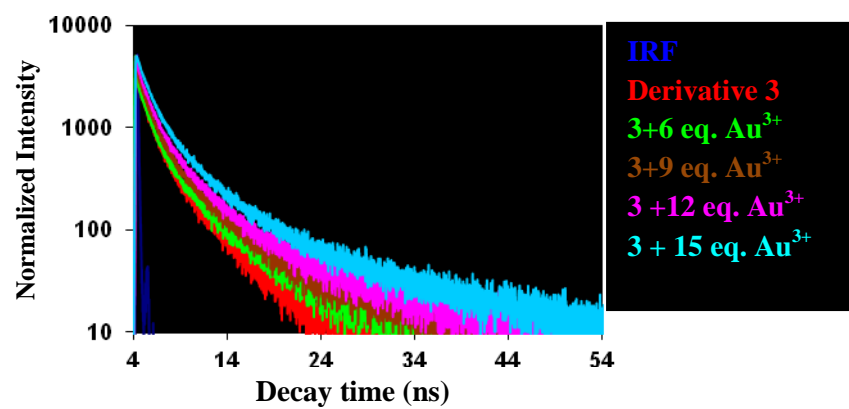


Fig. S13 Exponential fluorescence decays of **3** on addition of different amount of Au³⁺ ions measured at 485 nm. Spectra were acquired in H₂O/CH₃CN (6:4,v/v) mixture, λ_{ex} = 375 nm.

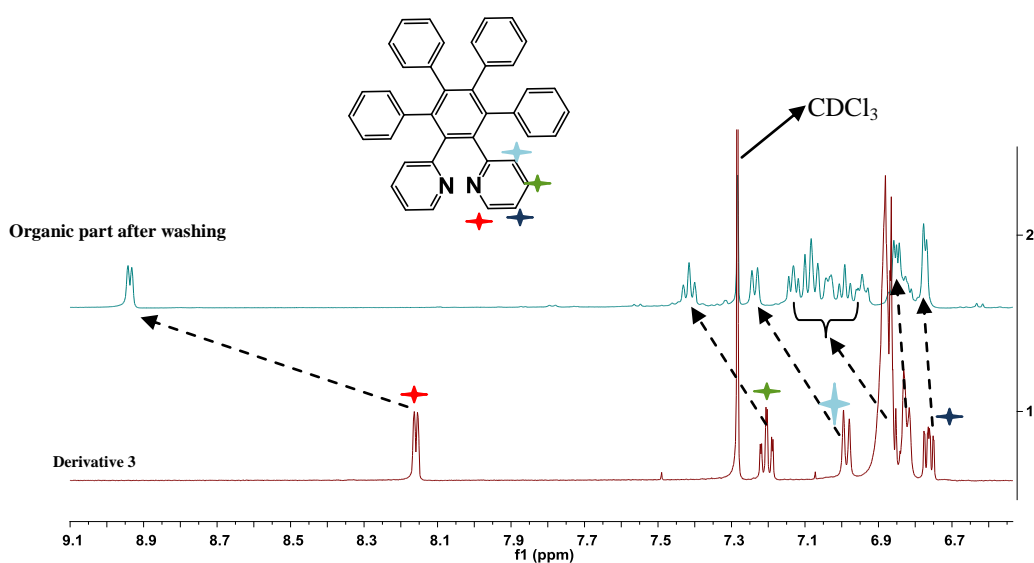


Fig. S14a Overlay ^1H NMR spectra of derivative **3** in CDCl_3 and organic part obtained after washing in-situ generated gold nanoparticles.

Derivative 3 (δ_1 ppm)	Organic part after treatment with gold (δ_2 ppm)	$\Delta\delta = \delta_1 - \delta_2$
8.16 (d, 2H, ArH) ★	8.95 (d)	0.79
7.20-7.28 (m, 2H, ArH) ★	7.39-7.42 (m)	0.14
6.99 (d, 2H, ArH) ★	7.21 (d)	0.22
6.88-6.82 (m, 20H, ArH)	Downfield splitting	-----
6.75-6.77 (m, 2H, ArH) ★	6.77-6.79	0.02

Fig. S14b Change in chemical shift (δ) value of compound **3** before and after formation of gold nanoparticles in CDCl_3 .

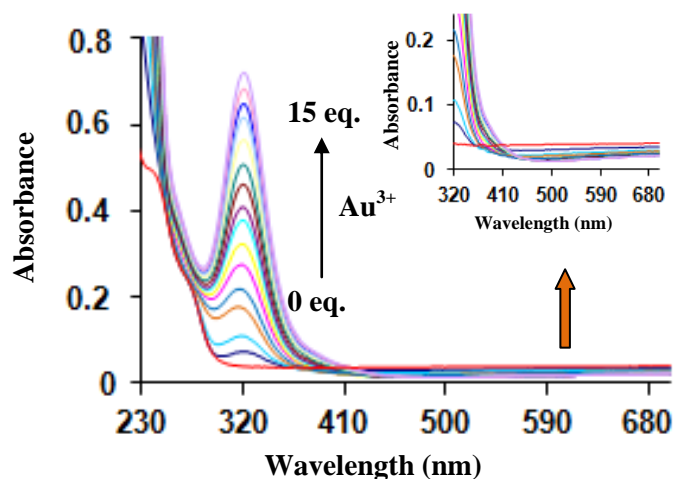


Fig. S15 UV-vis spectra of compound **3** (5 μM) upon additions of 15 eq. of Au^{3+} ions in CH_3CN . Inset showing no Surface Plasmon Resonance band was appeared around 550 nm.

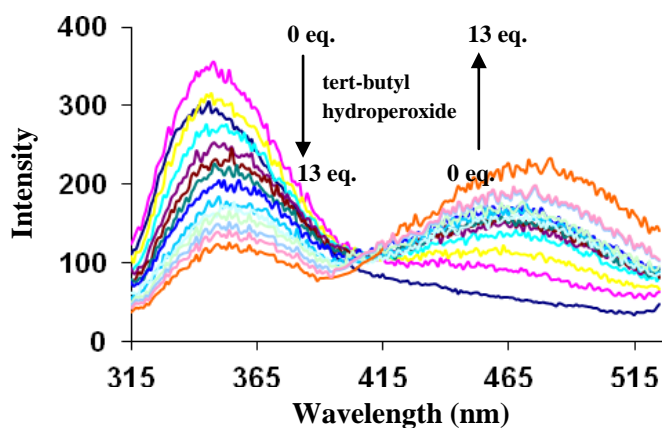


Fig S16 Fluorescence emission spectra of derivative **3** (5 μM) upon additions of 13 equiv. of 70 wt% tert-butyl hydroperoxide solution in $\text{H}_2\text{O}:\text{CH}_3\text{CN}$ (6/4) mixture.

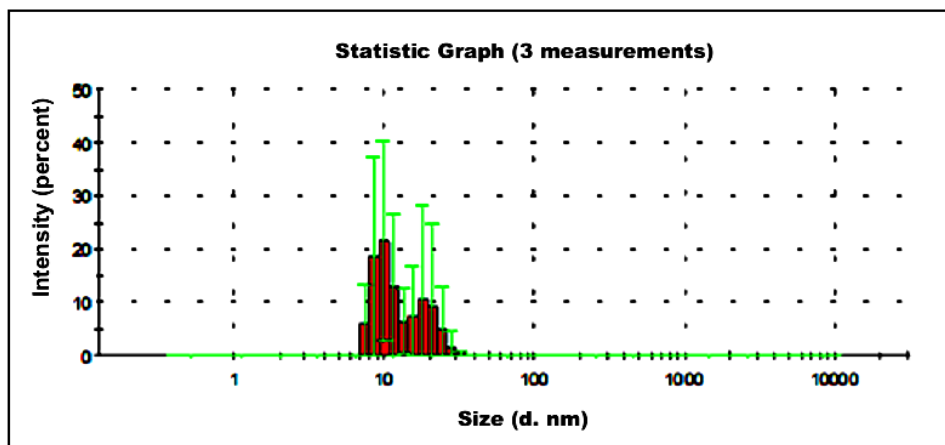


Fig. S17 The dynamic light scattering (DLS) studies of *in-situ* generated gold nanoparticles.

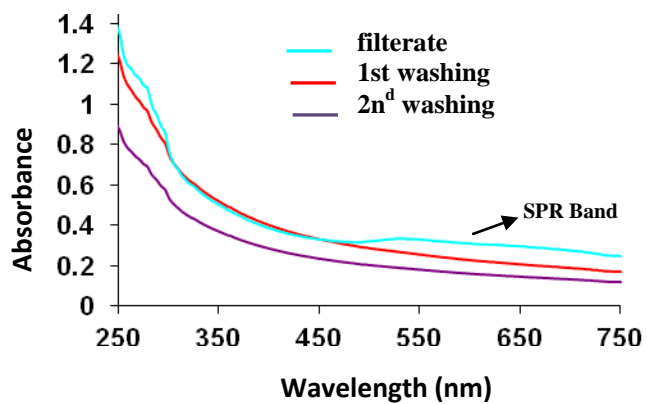


Fig. S18 Absorption spectra of the supernatants obtained subsequent washing steps in the preparation of AuNPs@MWCNTs nanohybrids.

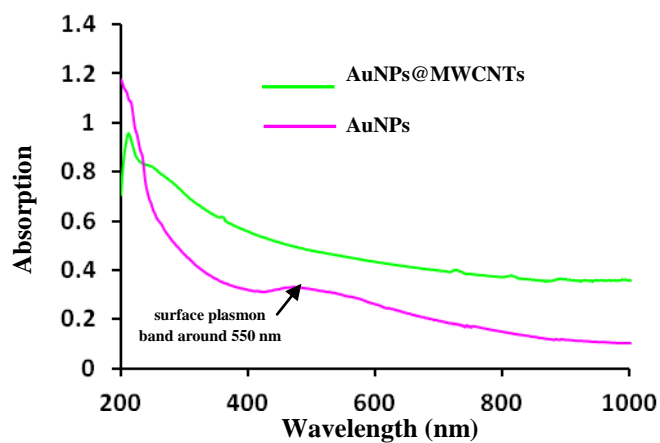


Fig. S19 UV-vis spectra of gold nanoparticles before and after they are adsorbed onto the surface of multi walled carbon nanotubes.

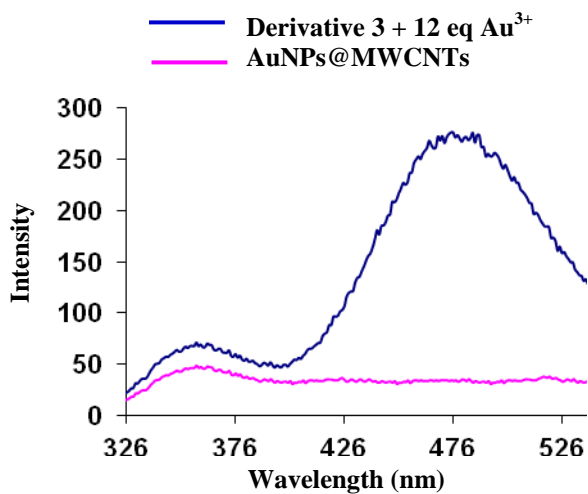


Fig S20 Fluorescence emission spectra of derivative **3** in presence of Au^{3+} and so prepared AuNPs@MWCNTs nanohybrid.

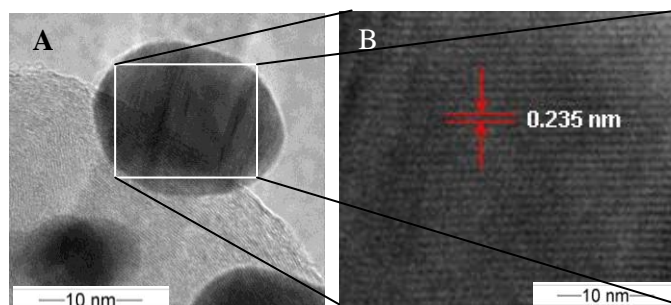


Fig. S21 (A) Magnified TEM images of AuNP@MWCNTs composites aligned Au NPs on the MWCNTs; (B) HRTEM of AuNPs decorated on MWCNTs.

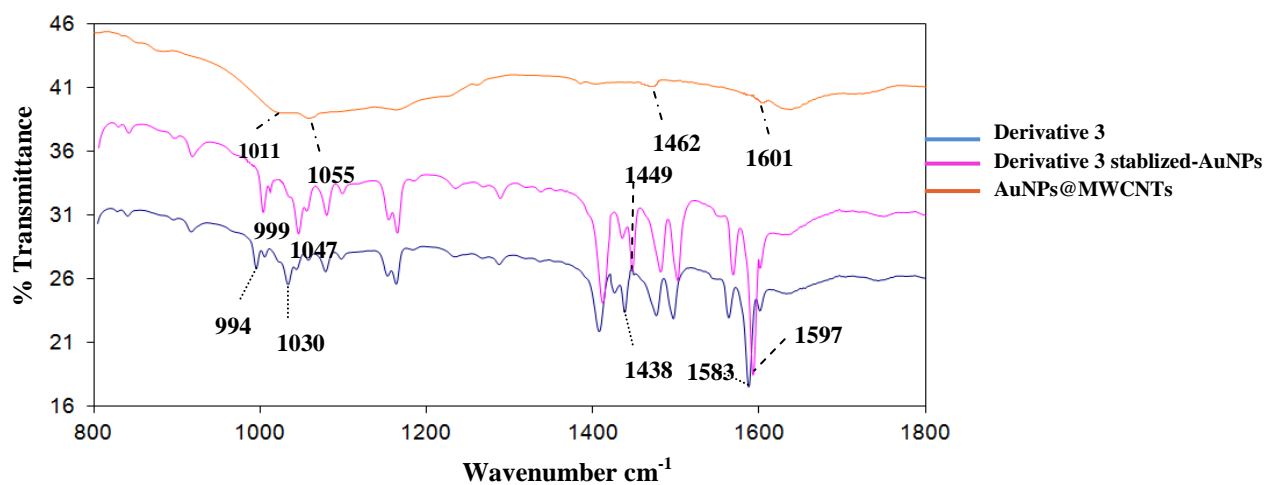


Fig. S22 The overlay FT-IR spectrum of derivative **3**, derivative **3** stabilized-AuNPs and AuNPs@MWCNTs hybrid material.

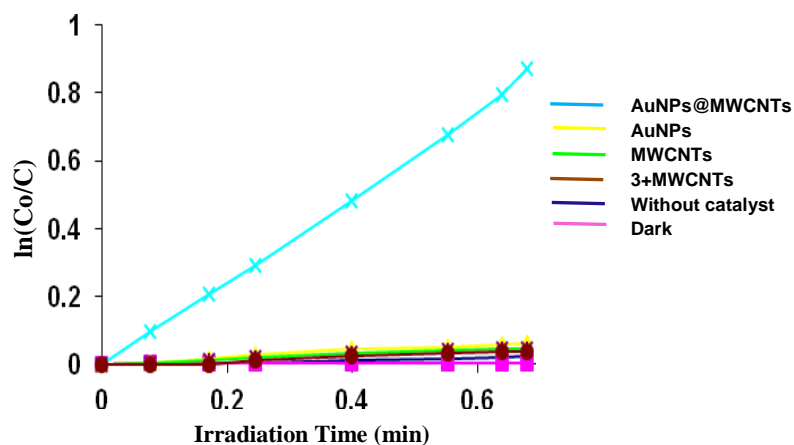


Fig. S23 The pseudo-first-order kinetic for the photodegradation of RhD B over AuNPs@MWCNTs, AuNPs, without catalyst and in dark.

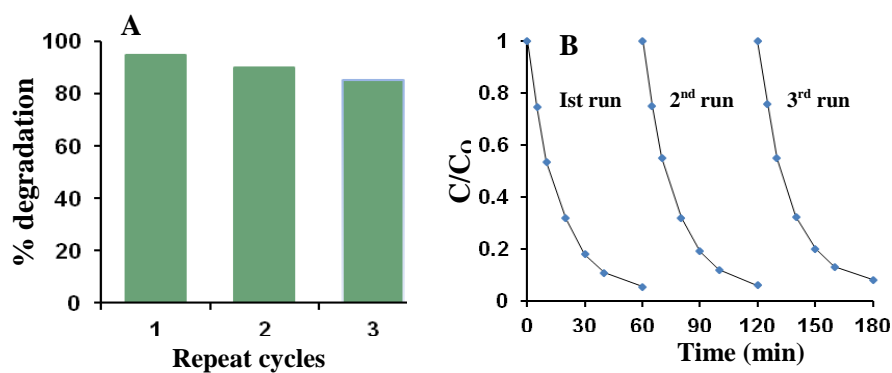


Fig. S24 (A) Dye adsorption efficiency and photocatalytic efficiency of the recycled AuNPs@MWCNTs nanocatalyst to RhB of separate 3 cycles of the continuous dark-adsorption and photocatalytic processes. (B) Repeated photocatalytic degradation of RhB on AuNPs@MWCNTs nanocatalyst under Visible light illumination.

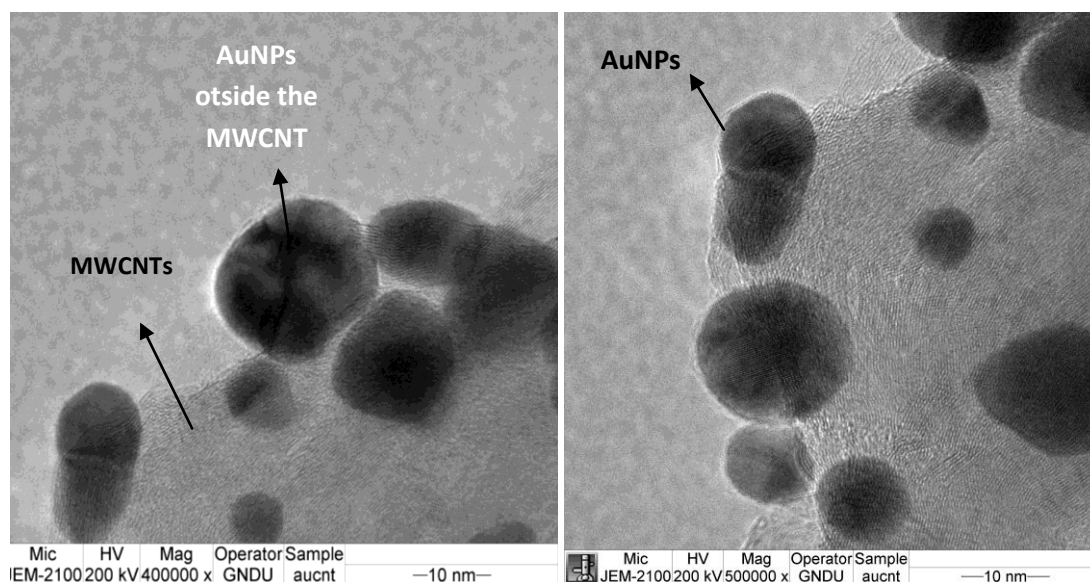


Fig. S25 TEM images of the AuNPs@MWCNTs nanohybrid catalyst after three runs of photocatalytic degradation of RhB.

Table S1: Fluorescence lifetime of derivative **3** in absence and presence of Au^{3+} ions (15 equiv) in $\text{H}_2\text{O}/\text{CH}_3\text{CN}$ (6:4, v/v) mixture at 485 nm. A_1 , A_2 , A_3 : fractional amount of molecules in each environment. τ_1 , τ_2 and τ_3 : biexponential life time of aggregates in 60 vol% of water in CH_3CN ; k_f : radiative rate constant ($k_f = \Phi/\tau_{\text{avg}}$); k_{nr} : nonradiative rate constant ($k_{\text{nr}} = (1 - \Phi)/\tau_{\text{avg}}$); $\lambda_{\text{ex}} = 375$ nm

Sample	Quantum Yield	$A_1/A_2/A_3$	τ_1 (ns)	τ_2 (ns)	τ_3 (ns)	τ_{avg} (Average lifetime, ns)	$k_f(10^9\text{s}^{-1})$	$k_{\text{nr}}(10^9\text{s}^{-1})$
Derivative 3	0.21	49.85/50.15	0.272	2.568	----	1.42	0.126	0.55
3+15 eq. Au^{3+}	0.32	51.16/26.74/22.10	3.531	0.919	17.470	5.91	0.05	0.116

Table S2: Comparison of present method for the preparation of AuNPs@CNTs nanohybrid materials over other reported procedure in literature.

S.No	Publication	Method of formation of AuNPs@CNTs nanohybrid	Reagent used	Reducing agent	Temp.	Total Time taken to prepare AuNPs@CNTs nanohybrid	Reusability
1.	Present Manuscript	Wet-chemical method	Derivative 3 in H ₂ O/CH ₃ CN, H ₂ SO ₄ , MWCNT and gold chloride	No	RT	Overnight	Yes
2.	Analyst, 2015, 140, 134–139	Frens' method	ammonium hydroxide, H ₂ SO ₄ , HNO ₃ , tetraethoxysilane), 3-aminopropyl-trimethoxysilane, 4-nitro thiophenol, Hydrogen tetrachloroaurate and MWCNT	trisodium citrate dihydrate	Room temp.	23 hrs	No
3.	Beilstein J. Nanotechnol. 2014, 5, 910–918	plasma enhanced chemical vapour deposition (PECVD)	VA-CNT, Ag paste, Pt resistor and Au wires	-----	170 °C	30 min	No
4.	ACS Sustainable Chem. Eng. 2013, 1, 746–752	layer-by-layer (LBL) assembly method	Polyethyleneimine, HAuCl ₄ , trisodium citrate and vertically aligned CNTs	trisodium citrate	100 °C	24 hr	No
5.	Nanoscale Research Letters 2014, 9:207	chemical vapor deposition	O ₂ /Ar atmosphere, HAuCl ₄ /2-propanol and CNT-AAO composite	-----	450 °C	26 hr	No
6.	J. Phys. Chem. C 2014, 118, 27028–27038	-----	Diocetylamine, tetraoctylammonium chloride, NABH ₄ , pyr-SH derivative, HAuCl ₄ and SWCNTs	NABH ₄	RT	overnight	No

Table S3: Comparison of catalytic activity of AuNPs@MWCNTs nanohybrid generated by utilizing derivative **3** for photocatalytic dye degradation of Rhodamine B under visible light source over other nanohybrid materials reported in literature.

S.No	Publication	Catalyst used	Time taken for dye degradation	Source of light used	Rate constant	reusability
1	Present manuscript	AuNP@MWCNTs	45 min	300 W tungsten lamp	0.066 min^{-1}	Yes
2	J. Am. Chem. Soc. 2015, 137, 2975–2983	Ti-Defected TiO_2 material	3 hr	300 W Xenon lamp	----	-----
2	ACS Appl. Mater. Interfaces 2015, 7, 4368–4380	TiO_2 materials	60 min	1000W Xe arc lamp	$0.0183 \times 10^{-3} \text{ min}^{-1}$	No
3	ACS Appl. Mater. Interfaces 2015, 7, 1616–1623	Au decorated $\text{ZnSe} \cdot 0.5\text{N}_2\text{H}_4$ Hybrid	240 min	500W Xe arc lamp	0.007 min^{-1}	No
4	DOI: 10.1021/jp5108679 J. Phys. Chem. C, 2015	$\text{BiF}_3\text{--Bi}_2\text{NbO}_5\text{F}$	90 min	300 W Xenon lamp	0.023 min^{-1}	Yes
5	J. Phys. Chem. C 2014, 118, 21447–21456	CdS nano structures	75 min	850 W xenon lamp	0.012 min^{-1}	No
6	ACS Appl. Mater. Interfaces 2014, 6, 613–621	graphene– SnO_2 aerosol nanocomposites	40 min	300 W xenon lamp ($\lambda > 420 \text{ nm}$)	0.091 min^{-1}	No
7	DOI: 10.1021/am507085u ACS Appl. Mater. Interfaces	Au-Decorated $\text{ZnSe} \cdot 0.5\text{N}_2\text{H}_4$ Nanowires	90 min	xenon lamp (500 W)	0.013 min^{-1}	No
8	DOI: 10.1021/sc5006473 ACS Sustainable Chem. Eng	A BiOBr/reduced graphene oxide (RGO) composite	5 hr	A 300 W Xe lamp	-----	Yes
9	Ind. Eng. Chem. Res. 2015, 54, 153–16	Graphene/MIL-53(Fe) composites	60 min	500W Xe arc lamp	0.07 min^{-1}	Yes
10	ACS Appl. Mater. Interfaces 2012, 4, 3084–3090	Graphene Oxide/ ZnO nano Composite	60 min	sunlight	-----	Yes
11.	DOI: 10.1021/acsami.5b00980 ACS Appl. Mater. Interfaces	ZnO:I/TiO_2 NRs	6 hr	500 W Xe lamp	-----	Yes